An all-sky survey at 230 GHz by MLS on Aura

Hugh C. Pumphrey [a,*] Richard E. Cofield [b] Mark J. Filipiak [a]
Nathaniel J. Livesey [b]

[a] *School of GeoSciences, The University of Edinburgh, West Mains Road, Edinburgh EH9 3JN, U.K.*

[b] *Mail stop 183-701, Jet Propulsion Laboratory, 4800 Oak Grove Drive, Pasadena, California, USA 91109-8099*

Abstract

The MLS instrument is a small satellite-borne radio telescope. Its purpose is to make limb-scanning measurements of atmospheric composition. One of the gases to which it is sensitive is carbon monoxide (CO), detected via the $J = 2 \rightarrow 1$ rotational transition at 230 GHz. CO is present in molecular gas clouds in the Milky Way. Although it was not designed for the purpose, MLS can detect emissions from galactic CO, allowing a map of the 230 GHz radio sky to be constructed. We report the MLS measurements of galactic radio emission and discuss their effect on the atmospheric mission of MLS. The region of the Milky Way with emissions strong enough to significantly affect MLS observations of atmospheric CO is identified. Ground-based radio astronomers have been mapping the sky using CO emission for many years. However the MLS data are the first such survey to be carried out from space. The MLS survey covers a larger area of the sky than any other 230 GHz survey, but no previously unknown gas clouds are observed.

Key words: galaxy, CO, radio-astronomy, MLS, limb-sounding, stratosphere

* Corresponding author
Email addresses: H.C.Pumphrey@ed.ac.uk (Hugh C. Pumphrey),
Richard.E.Cofield@jpl.nasa.gov (Richard E. Cofield),
M.J.Filipiak@ed.ac.uk (Mark J. Filipiak),
Nathaniel.J.Livesey@jpl.nasa.gov (Nathaniel J. Livesey).

1 Introduction

The Microwave Limb Sounder (Waters et al., 2006), or MLS, is one of four instruments on NASA's Aura satellite (Schoeberl et al., 2006): a mission whose purpose is to study the chemistry of the Earth's atmosphere. MLS is essentially a radio telescope. Its 2 m dish antenna feeds several heterodyne radiometers, the output of which is analysed by spectrometers consisting of banks of filters. Each filter bank is located at the frequency of a rotational transition of a target molecule; these molecules include H_2O, ClO, O_3, HNO_3 and CO.

The MLS antenna views in the plane of the satellite's orbit, looking forward from the satellite. The antenna is tilted so that its field of view scans across the Earth's limb, the tangent point moving from an altitude near 0 km to one near 95 km during the course of one scan. A total of 3495 such scans are made during the course of one day. In the upper portion of the scan, the atmosphere is entirely transparent at the frequencies of most of the MLS channels, so that the instrument is observing radiation from space. In most MLS bands there is no extra-terrestrial signal to be observed above the MLS noise level. However the signal from space in the carbon monoxide (CO) band at 230 GHz is observable: it is these observations that we report in this paper.

Most signals from space due to CO have their origin in clouds of molecular gas lying in or near the plane of the Milky Way Galaxy. CO is the second commonest molecule in these clouds after H_2 and hence the commonest molecule with a dipole moment. Radio astronomers have been aware of this for many decades and have used the CO signal to map the galaxy in considerable detail. Usually the $J = 1 \rightarrow 0$ transition at 115 GHz has been used (See Dame et al. (2001) and references therein) but the $J = 2 \rightarrow 1$ line has also been used (Oka et al., 1996).

2 The nature of the data

2.1 Spectral coverage

The $J = 2 \rightarrow 1$ transition of CO has a frequency of 230.538 GHz. Of MLS's five radiometers, the one that concerns us here has a local oscillator frequency of 239.66 GHz. The filter bank centred on the CO line is positioned 9.116 GHz from the local oscillator, so that it is sensitive to incoming radiation at 248.776 GHz in the upper sideband and 230.544 GHz in the lower sideband. The satellite's orbital velocity of 8 km/s causes terrestrial emission

at 230.538 GHz to be Doppler-shifted to 230.544 GHz as it arrives at the radiometer. The CO filter bank is therefore effectively centred on the frequency of the CO line as observed in the Earth's frame of reference. MLS is a double-sideband instrument, so the measurements contain roughly equal contributions from each sideband.

The filter bank consists of 25 filters with widths varying from 6 MHz (7.8 km/s Doppler shift) in the band centre to 96 MHz (125 km/s) at the edges, giving a total bandwith of about ±600 MHz (±780 km/s). This design was chosen to accommodate the pressure broadening of atmospheric spectral emissions: the pressure-broadened linewidth is about 300 MHz at the tropopause, decreasing with height to reach a value smaller than the Doppler linewidth at the mesopause. Gas clouds in the Milky Way are at far too low a pressure to exhibit pressure broadening, but have large line-of-sight velocities. The largest velocities observed are on the order of 300 km/s so the filter bank is able to observe the entire range of Doppler shifts. The spectral resolution, however, is much poorer than that of modern ground-based instruments.

The radiometer operates at ambient temperature. This, together with an integration time of 1/6 s, leads to a measurement noise of 0.94 K on an individual measurement in the 8 MHz-wide channels near the band centre. In the 64 MHz-wide channels which are sensitive to the galactic signals with the largest Doppler shifts, the noise on an individual measurement is 0.38 K. This noise level is quite adequate for the instrument's limb-sounding mission, but is rather large for serious astronomical work.

2.2 Sky coverage

The Aura satellite is in a circular, sun-synchronous orbit at an altitude of 705 km. The inclination of the orbit is 98°, i.e. it is a retrograde orbit which passes within 8° of the poles. As the MLS field of view lies in the orbital plane, the tangent point passes through all latitudes between 82°N and 82°S on every orbit. As a consequence, the point on the celestial sphere observed by MLS passes through all declinations between 82°N and 82°S on every orbit. The rotation of the Earth causes the track of the tangent point across the Earth on consecutive orbits to be separated by 24° of longitude. However, as the Aura orbit is sun-synchronous, the angle between the orbit plane and the Earth-Sun line remains constant. As a result, the track of the field of view across the celestial sphere changes only slightly between one orbit and the next. The end result is that the whole celestial sphere (with the exception of an 8° circle around each pole) is observed twice per year: once from the half of the orbit where the declination of the field of view is increasing and once from the half where it is decreasing.

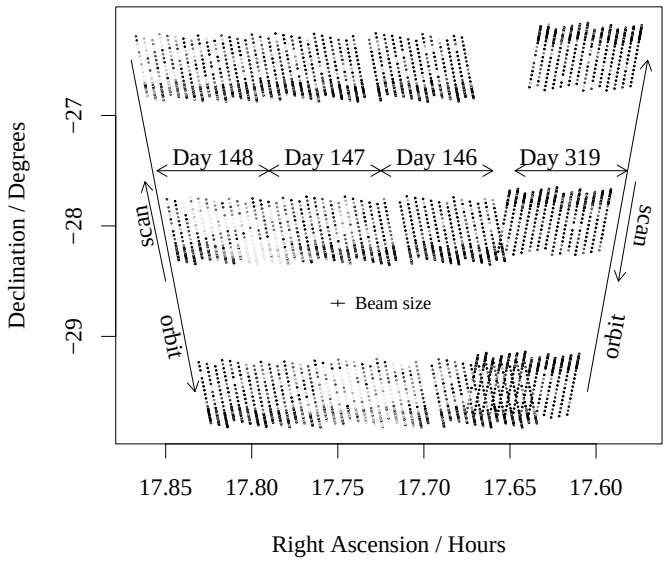

Fig. 1. A region of the sky close to the galactic centre. Each dot marks the position of a single MLS observation. Only observations with a tangent altitude above 50 km are shown. The palest dots indicate a brightness temperature above 4 K in channel 15 of the MLS CO band; brightness temperatures near or below zero are black.

The MLS scan is not made at a constant speed: of the 120 measurements recorded during a single scan, the majority are made with the tangent point in the troposphere and lower stratosphere. The scan across the upper stratosphere and lower mesosphere is faster, and that across the upper mesosphere is faster again. This design is based on MLS's main science goals, most of which relate to the lower stratosphere and upper troposphere. For tangent heights greater than 50 km, no signal from the atmosphere is observed in any channels in the CO band except the centre three channels. The two channels either side of the centre channel have a clear view to space over a more restricted range of tangent heights: typically above 70 km. The line centre channel never gets a clear view to space when MLS is operating in its usual manner.

The locations of observations with a clear view to space on a section of the celestial sphere are shown in figure 1. Three consecutive days observations are shown, together with one day from six months later, at which time the same region of the sky is viewed from the other side of the orbit. Note how the coverage is reasonably dense in strips at a fixed declination: this is because the MLS scan is synchronised with the Aura orbit. When the same region is viewed one year later, the orbits will be at slightly different right ascensions so that the density of observations in the observed strips will increase. But the gaps between these strips never get filled in, except for rare occasions when MLS operates in a non-standard scanning mode. The field of view has a beamwidth (full width at half power) of 0.06° in the direction along the scan and 0.12° across it — this is indicated by a small cross on figure 1. Within the observed strips the observation density is well matched to the beam width.

3 Results

3.1 Coarse resolution survey

Figure 2 shows the MLS view of the sky, averaged over the period August 2004 to May 2008. The data are averaged into boxes 1.5° of declination by 4 minutes (1° angle) of right ascension; if a significantly finer grid were chosen then many boxes would contain few or no data. Many of the known features of the galaxy, as shown in figure 2 of Dame et al. (2001), may be seen in figure 2. The central region of the galaxy is the most obvious. Springing from this is the triangular Aquila rift at a galactic longitude l of 30°. There are bright patches on the galactic equator in Cygnus near $l = 90°$ and in Carina/Vela near $l = 270°$. Further away from the galactic centre the clouds are less bright and spread over a wider range of galactic latitude b. Examples south of the galactic equator are the Orion complex near $l = 210°$ and the Taurus/Perseus/Auriga complex between $l = 180°$ and $l = 150°$. North of the galactic equator lie the Polaris and Cepheus flares near $l = 110°$.

The data contain a few non-astronomical artifacts, despite concerted efforts to filter them out. Some of these can be identified as such because they lie along the track of the orbits: an example in the upper panel of figure 2 may be seen crossing the galactic equator near $l = 12$. Also in the upper panel there is a sinusoidal feature lying between declinations of ±23°. This occurs at the point where the spacecraft crosses the terminator from night to day and is thought to be an effect of the sudden exposure of the instrument to sunlight.

Figure 2 suppresses the Doppler shift information in order to show both dimensions of the sky in a single figure. In order to present the Doppler shift information, we re-average the data into a 1.5° $l - b$ grid and plot only data within 3° of the galactic equator; the results are shown in figure 3. The MLS measurements have a slight systematic error which varies from channel to channel and changes little with time. For the purposes of figure 3 this was removed by subtracting an average spectrum for a region of sky well away from the galaxy and then adding a constant brightness temperature of 0.189 K representing the radiance from a black body at a temperature of 2.73 K. Again, many of the known features (see figure 3 of Dame et al. (2001)) of the galaxy are visible; some are identified in the lower panel of the figure. There are two clear differences between the data from the two sides of the orbit. Firstly, the upper panel has features appearing at $l = 10$ and $l = -170$. These occur where the non-astronomical sinusoidal feature in the upper panel of figure 2 crosses the galactic plane. Secondly, the galactic signal in the upper panel of figure 3 appears at a larger line-of-sight velocity. This is due to the motion of the Earth around the sun. Earth's orbital velocity v_o is about $30\,\mathrm{km\,s^{-1}}$, but

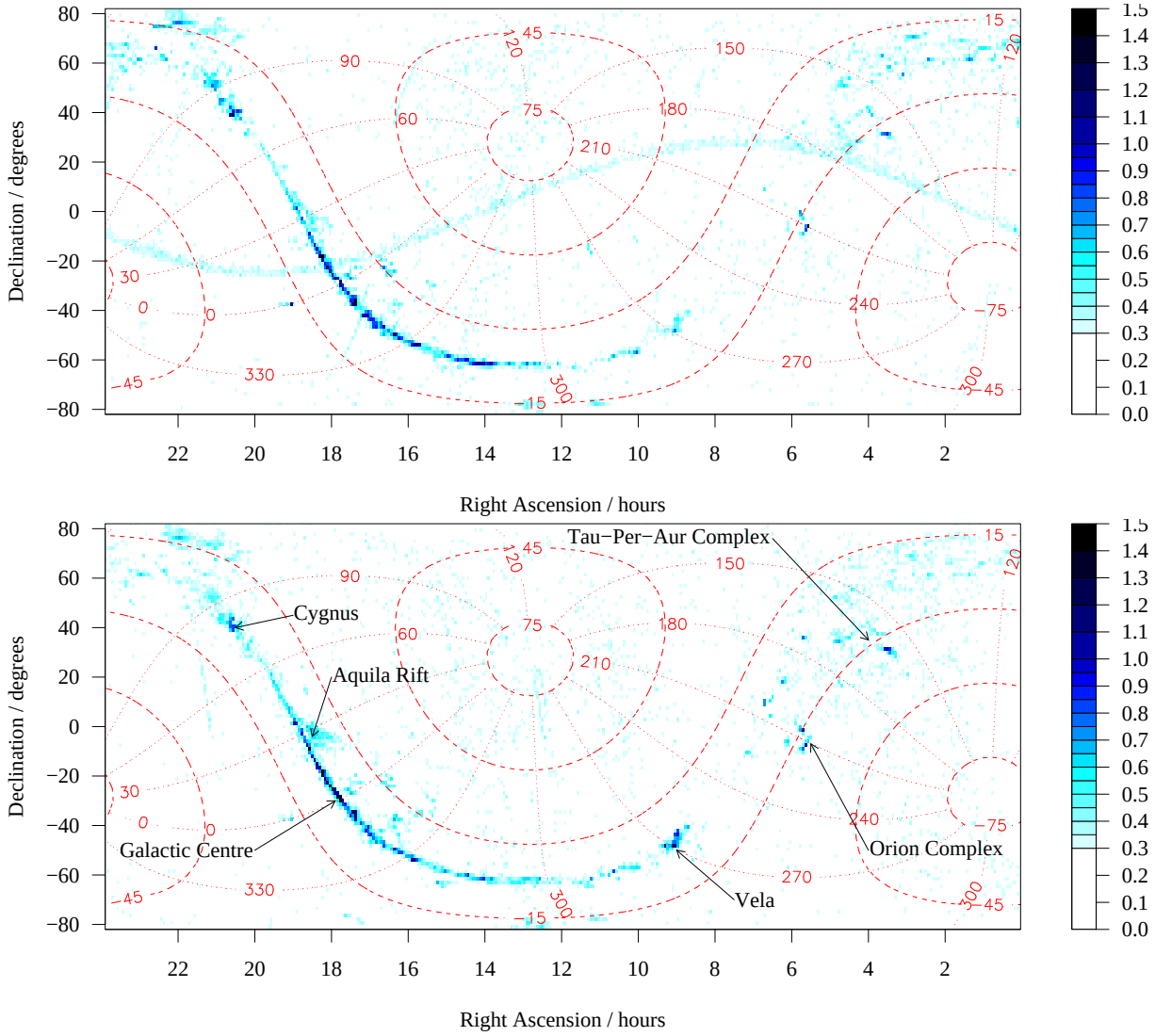

Fig. 2. Radio sky as observed by MLS. The quantity shown is brightness temperature in K, in whichever MLS channel has the largest brightness temperature. The dotted and dashed grid lines are lines of constant galactic longitude, l, and galactic latitude, b, respectively. Upper panel shows radiances from the half orbits for which the FoV has increasing declination. Lower panel shows radiances from the half orbits for which the FoV has decreasing declination.

the angle $\chi = 22.5°$ between the orbital plane and the Earth-Sun line gives v_o a maximum component along the MLS line of sight of $v_o \sin\chi \approx 11\,\mathrm{km\,s^{-1}}$. We can therefore expect the Doppler shifts observed on the two sides of the orbit to differ by a maximum of $22\,\mathrm{km\,s^{-1}}$, more or less as observed. A more detailed treatment of the geometry would permit the data from the two sides of the orbit to be corrected to the local standard of rest and hence combined to form a slightly improved data set. Most of the differences between the galactic signals shown in the two panels of figure 2 are due to the Doppler shift from the Earth's orbit combined with the limited spectral resolution and the fact

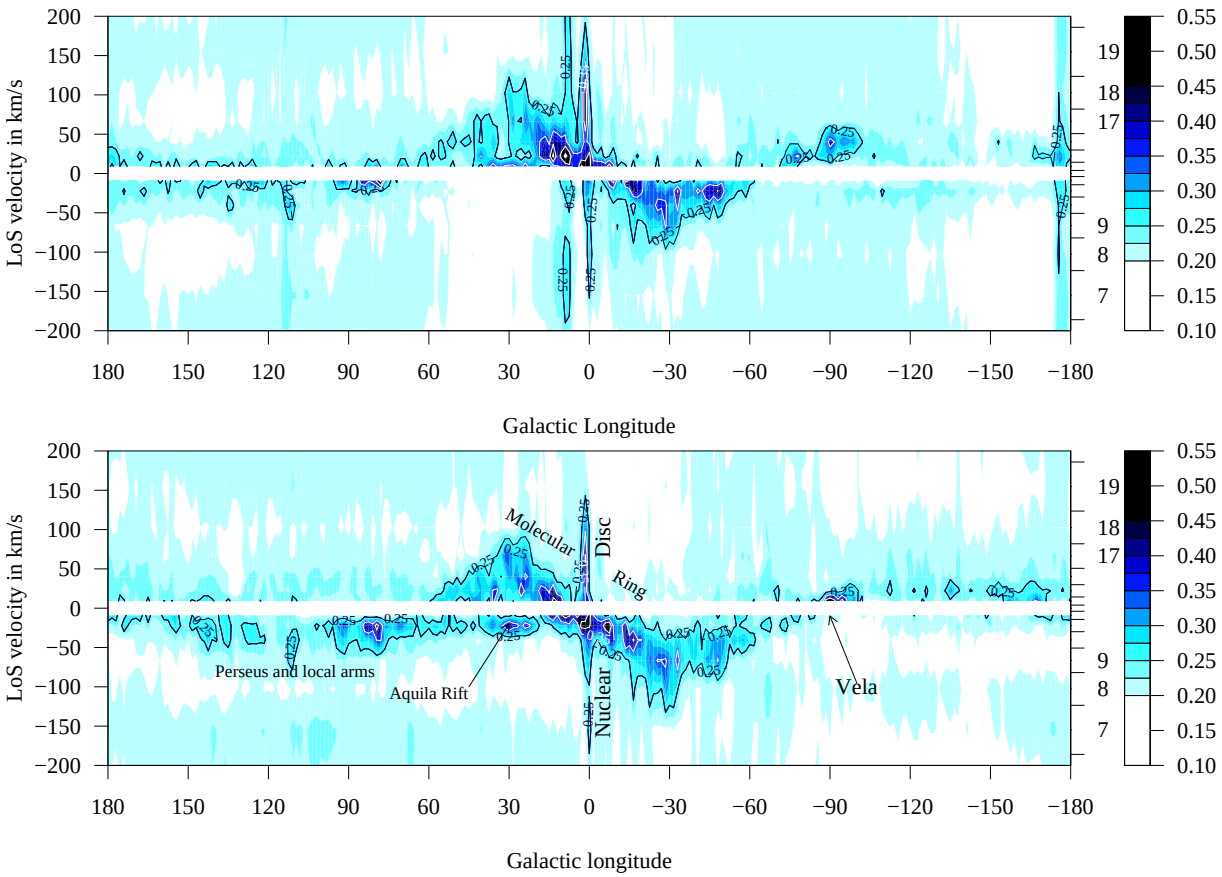

Fig. 3. Longitude-velocity plots for data within 3° of the galactic equator. The right-hand axis shows the numbers and edges of the MLS channels. Channels 1-6 and 20-25 are not shown as they correspond to larger Doppler shifts than are present in the Milky Way. Positive velocities are towards the instrument. Upper panel shows radiances from the half orbits for which the FoV has increasing declination, lower panel shows radiances from the half orbits for which the FoV has decreasing declination

that a clear view of space is not obtained in the band centre channel.

We make a quantitative comparison between the MLS data and ground-based 115 GHz observations by showing mean spectra for three regions: the galactic core, the Aquila rift region near $b = 27°$ and the Cygnus region near $b = 80°$. The 115 GHz data are those described in Dame et al. (1987); these data were obtained from the Astronomical Data Center (http://adc.gsfc.nasa.gov). In order to compare the two datasets it was necessary to process the MLS data slightly. As with figure 3 we subtracted a spectrum from a signal-free region of the sky. We then divided the result by the MLS sideband fraction for the lower sideband. The resulting data are shown in figure 4; they agree reasonably well with the 115 GHz observations. Both sets of observations show narrower spectra at greater distances from the galactic centre. The intensities of the two transitions are similar near the galactic centre, but the 230 GHz intensity

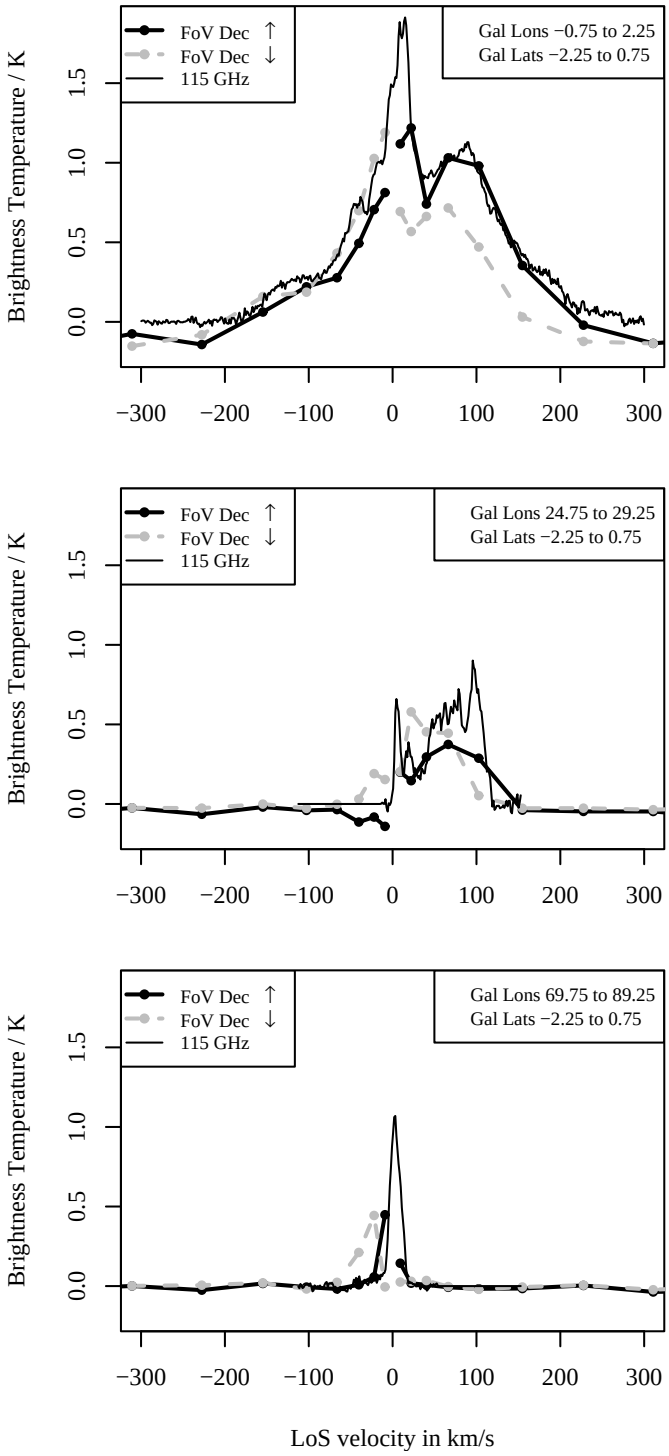

Fig. 4. MLS 230 GHz and ground-based radio-telescope 115 GHz spectra for three regions of the galaxy: the core (top), the Aquila rift region (centre) and the Cygnus region (bottom)

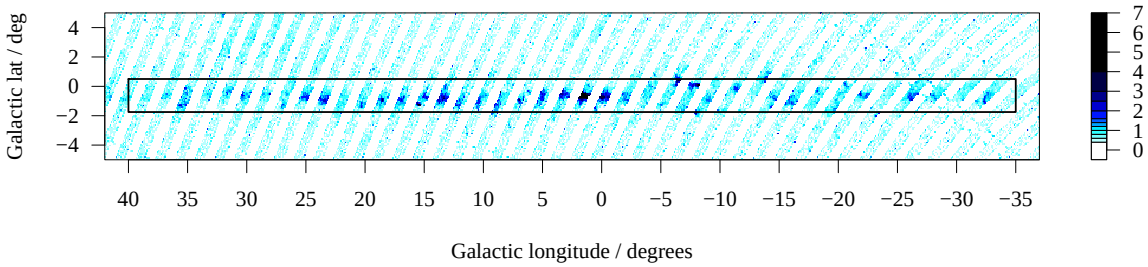

Fig. 5. Radiances from the half orbits for which the FoV has decreasing declination. The region within the rectangle is deemed to have a serious effect on the atmospheric CO measurement, as described later in the text.

is considerably smaller for larger values of $|l|$. This is in rough agreement with other 230 GHz observations such as those of Oka et al. (1996), which give values for the CO($2 \rightarrow 1$)/CO($1 \rightarrow 0$) ratio of 0.75 for much of the galaxy, but values > 1 in the core region.

3.2 Galactic core

Figure 5 shows the galactic core region. The data are averaged into 0.1° boxes in galactic co-ordinates and, as in figure 2, the brightness temperature shown is that from whichever channel had the greatest brightness temperature in each grid box. Considerable detail in the galactic core region can be seen; this detail is in reasonable agreement with figure 2 of Dame et al. (2001).

4 Effect of galactic emission on atmospheric retrieval

The MLS observations do not reveal anything unexpected about the galaxy. It was, however, necessary to examine them in some detail in order to properly understand the effect that the galactic radiances have on the measurement of atmospheric CO. It was realised early in the mission that the CO data were contaminated by radiance from the galaxy. In the current data version, v2.2, (Pumphrey et al., 2007) the intention was that affected data would be flagged as such. Unfortunately, a software error prevented this and users of the data need to be aware of the presence of the contaminated data and to avoid using it. Figure 6 shows zonal mean CO mixing ratio for the worst-affected altitude. The corresponding sky radiances are shown in the same co-ordinate system for comparison. The effect of the galaxy on the CO mixing ratios can be seen as a narrow band of slightly elevated values which appear at the same dates and latitudes as the brightest parts of the galaxy. The galactic core appears as small regions of considerably enhanced values near 60°N around day 147 of the year and near 60°S around day 321.

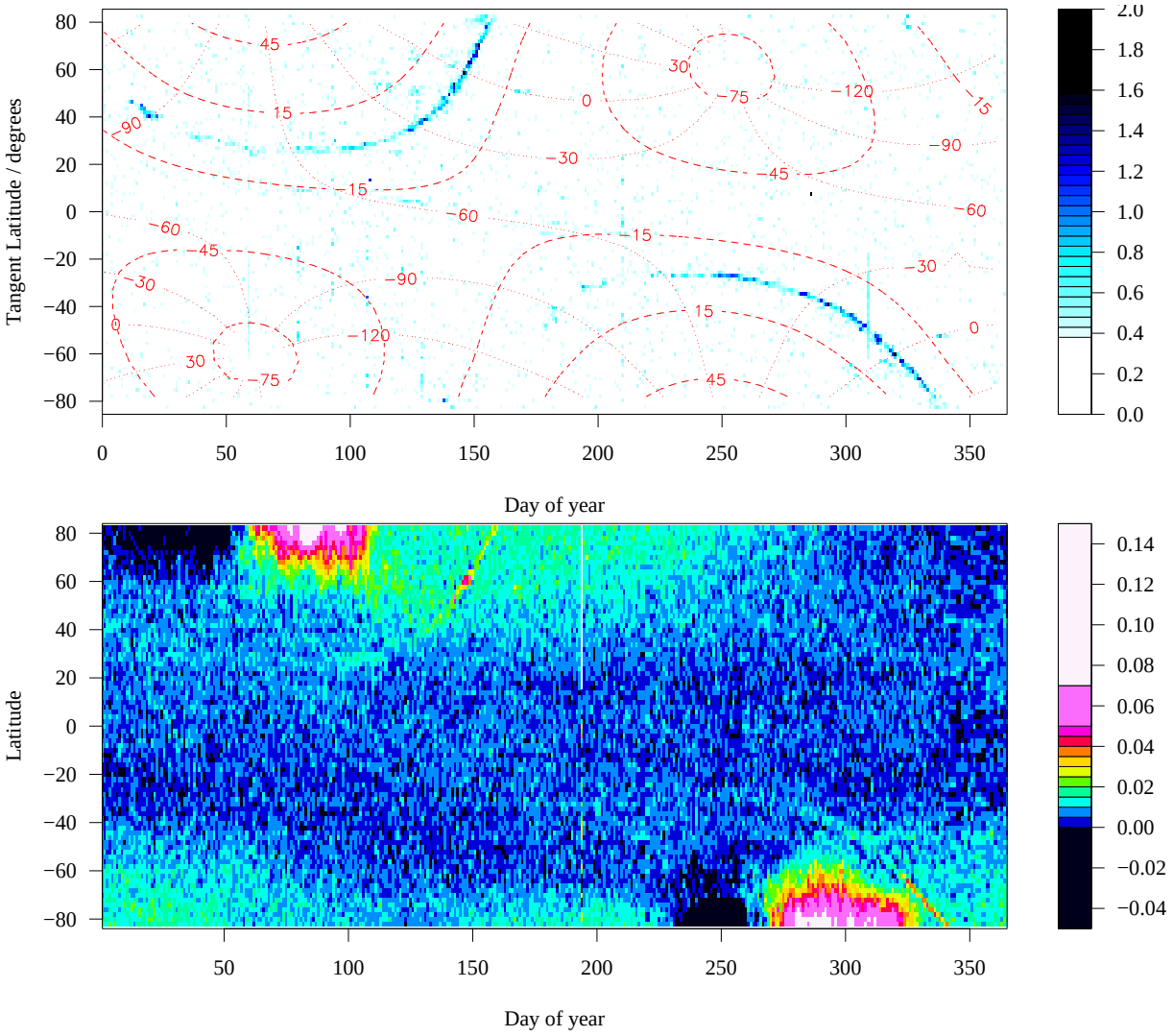

Fig. 6. Upper panel: Radiances from the descending half-orbits (those for which the *tangent point* has decreasing latitude). The dotted and dashed grid lines are lines of constant l and b respectively. Lower panel: MLS zonal mean CO VMR in parts per million by volume (ppmv) for 2007. Data shown are for an atmospheric pressure of 22 hPa (approximately an altitude of 27 km): the data for this level in the atmosphere are more affected by the galactic radiances than any other level.

It is perhaps surprising at first that the galactic contamination should have the most obvious effect on the data for the lower stratosphere. However, at higher altitudes, both the mixing ratio of CO and the error on the MLS measurement of it become much larger, so the galactic perturbation becomes negligible in relative terms.

As figure 1 shows, MLS observes the galactic core on approximately day 147 and on day 321 of each year. Both observations occur on the side of the orbit where the tangent point latitude is decreasing (the descending side) — note that Pumphrey et al. (2007) state incorrectly that the day 321 observation

occurs on the ascending side. The CO data is affected for a number of days either side of the core observation, but the galactic radiances can be observed over a much wider range of days. As figure 3 shows, regions of the galaxy separated from the core by more than 30° of longitude have small Doppler shifts and affect only a few MLS channels. Regions closer to the core than this have large Doppler shifts and affect a larger number of MLS channels, including those used to retrieve CO in the (CO-poor) stratosphere. For this reason, in the forthcoming version of the MLS data (v3), all radiances from MLS's CO bands will be rejected if $-35° < l < 40°$ and $-1.75° < b < 0.5°$. This region is marked in figure 5.

5 Summary

Data from MLS on Aura have been used to map the radio sky in the 230 GHz band. The observed distribution agrees qualitatively with ground-based observations, both in the location and the Doppler shift of the observed clouds. The effect of the radiances from space on the estimated atmospheric CO mixing ratio has been quantified. A criterion has been decided on for decreeing a measurement to be unsuitable for atmospheric CO retrievals.

MLS was not designed for radio astronomy. However the concept of a radio telescope on a satellite is a useful one, as demonstrated by the Odin mission (see Hjalmarson et al. (2005) and references therein.) The main deficiencies of MLS for an astronomer are its high noise level and its non-uniform spectral resolution. The latter was a design choice driven by the MLS science goals: a different sort of spectrometer would be chosen for a mission with astronomical goals. The Odin mission is an example which has already produced many results. In future missions it will be possible to obtain far lower noise by the use of supercooled receivers. The JEM-SMILES limb sounding mission (see http://smiles.tksc.jaxa.jp/), to be flown in the near future on the International Space Station, will demonstrate the feasibility of this technology for space use.

References

Dame, T. M., Hartmann, D., Thaddeus, P., February 2001. The Milky Way in molecular clouds: a new complete CO survey. The Astrophysical Journal 547, 792–813.

Dame, T. M., Ungerechts, H., Cohen, R. S., de Geus, E. J., Grenier, I. A., May, J., Murphy, D. C., Nyman, L. A., Thaddeus, P., Nov 1987. A composite co survey of the entire milky way. Astrophysical Journal 322, 706–720.

Hjalmarson, A., Bergman, P., Biver, N., Floren, H.-G., Frisk, U., Hasegawa, T.,

Justtanont, K., Larsson, B., Lundin, S., Olberg, M., , Olofsson, H., Persson, G., Rydbeck, G., Sandqvist, A., 2005. Recent astronomy highlights from the Odin satellite. Adv. Space Res. 36, 1031–1047.

Oka, T., Hasegawa, T., Handa, T., Hayashi, M., Sakamoto, S., 1996. CO ($J = 2 - 1$) line observations of the galactic center molecular cloud complex. I. On-plane structure. Astrophysical Journal 460, 334–342.

Pumphrey, H. C., Filipiak, M. J., Livesey, N. J., Schwartz, M. J., Boone, C., Walker, K. A., Bernath, P., Ricaud, P., Barret, B., Clerbaux, C., Jarnot, R. F., Kovalenko, L. J., Manney, G. L., Waters, J. W., 2007. Validation of middle-atmosphere carbon monoxide retrievals from MLS on Aura. Journal of Geophysical Research 112, D24S38, doi:10.1029/2007JD00872.

Schoeberl, M. R., Douglass, A. R., Hilsenrath, E., Bhartia, P. K., Barnett, J., Beer, R., Waters, J., Gunson, M., Froidevaux, L., Gille, J., Levelt, P. F., DeCola, P., May 2006. Overview of the EOS Aura mission. IEEE Trans. Geosci. Remote Sensing 44 (5), 1066–1074.

Waters, J. W., Froidevaux, L., Harwood, R., Jarnot, R., Pickett, H., Read, W., Siegel, P., Cofield, R., Filipiak, M., Flower, D., Holden, J., Lau, G., Livesey, N., Manney, G., Pumphrey, H., Santee, M., Wu, D., Cuddy, D., Lay, R., Loo, M., Perun, V., Schwartz, M., Stek, P., Thurstans, R., Boyles, M., Chandra, S., Chavez, M., Chen, G.-S., Chudasama, B., Dodge, R., Fuller, R., Girard, M., Jiang, J., Jiang, Y., Knosp, B., LaBelle, R., Lam, J., Lee, K., Miller, D., Oswald, J., Patel, N., Pukala, D., Quintero, O., Scaff, D., Snyder, W., Tope, M., Wagner, P., Walch, M., May 2006. The Earth Observing System Microwave Limb Sounder (EOS MLS) on the Aura satellite. IEEE Trans. Geoscience and Remote Sensing 44 (5), 1106–1121.